ResearchGate

See discussions, stats, and author profiles for this publication at: https://www.researchgate.net/publication/235931622

Tuning the Molecular Properties of Polybenzimidazole by Copolymerization

DATASET · JANUARY 2007

CITATIONS
17

READS
48

4 AUTHORS, INCLUDING:

Arindam Sannigrahi
Pidilite Industries Ltd
17 PUBLICATIONS **331** CITATIONS
SEE PROFILE

Arunbabu Dhamodaran
McGill University
13 PUBLICATIONS **267** CITATIONS
SEE PROFILE

Available from: Murali Sankar Rajavelu
Retrieved on: 26 January 2016

Tuning the Molecular Properties of Polybenzimidazole by Copolymerization

Arindam Sannigrahi, Dhamodaran Arunbabu, R. Murali Sankar, and Tushar Jana*

School of Chemistry, University of Hyderabad, Hyderabad, India

Received: May 23, 2007; In Final Form: August 14, 2007

In the present work, a series of novel random polybenzimidazole (PBI) copolymers consisting of *m*- and *p*-phenylene linkages are synthesized from various stoichiometric mixtures of isophthalic acid (IPA) and terephthalic acid (TPA) with 3,3′,4,4′-tetraaminobiphenyl (TAB) by solution copolycondensation in polyphosphoric acid (PPA). The resulting copolymers are characterized by different techniques to obtain their molecular properties parameters. The monomer concentration in the polymerization plays an important role in controlling the molecular weight of the polymer. Surprisingly, a simple change in the dicarboxylic acid architecture from meta (IPA) to para (TPA) increases the molecular weight of the copolymers, which is maximum for the para homopolymer. The low solubility of TPA in PPA is found to be the dominating factor for obtaining the higher molecular weight polymer in the case of the para structure. FT-IR study shows that the introduction of the para structure enhances the conjugation along the polymer chain. The positive deviation of the copolymer composition from the feed ratio is due to the higher reactivity ratio of TPA than IPA, which is obtained from proton NMR studies. The incorporation of the para structure in the chain enhances the thermal stability of the polymers. The para homopolymer shows 59 °C lower glass transition temperature compare to the meta homopolymer indicating enhancement of the flexibility of the polymer chain due the introduction of the *p*-phenylene linkage in the backbone. The T_g of the copolymers shows both positive and negative deviation from the expected T_g calculated by the Fox equation. The enhanced conjugation of the polymer chains also influences the photophysical properties of the polymers in solution. All the PBI polymers exhibit strong fluorescence in dimethylacetamide solution. As expected, that all the polymers are amorphous in nature reveals that the copolymerization does not influence the packing characteristics of the PBI chains.

1. Introduction

The fuel cell is the most promising electrochemical device for the production of an efficient, environment-friendly, and economical power energy.[1] A polymer electrolyte membrane fuel cell (PEMFC) employing a solid polymer electrolyte to separate the fuel from the oxidant has received a great deal of attention due to its potential as a high energy density power generator.[2] The most widely used perflurosulfonic acid (PFSA) based polymer membrane such as Dupont's Nafion has severe limitations:[3] (1) proton conduction requires a water solvated membrane, (2) low operating temperature, and (3) high cost. However, a high-temperature polymer electrolyte membrane (HT-PEM) operating above 120 °C overcomes the above-mentioned problems and offers many advantages which include fast electrode kinetics, high tolerance to fuel impurity, etc.[4] Hence, proton conducting polymers with superior thermochemical and mechanical stability above 120 °C have been strongly desired for PEMFC application.

Until now, a large number of various high-temperature polymer electrolyte membranes have been developed and reviewed.[5−8] Polybenzimidazole (PBI, Scheme 1) has excellent thermal and chemical resistance, fire retarding capacity, and insulating property and it forms a good textile fiber.[9] Phosphoric acid (PA) doped polybenzimidazole (PBI) has emerged as a promising candidate for a low-cost and high-performance fuel cell material.[10,11] PBI possesses both proton donor (−NH−) and proton acceptor (−N═) hydrogen-bonding sites which exhibit specific interaction with the polar solvents[12−14] and form miscible blends[15,16] with a variety of polymers. PBI is being used for various purposes especially for high-temperature application, fiber spinning, and as a reverse osmosis membrane, fluorescence sensor for halide ions, etc.[9,17] A variety of approaches have been explored to prepare the PA-doped PBI membrane such as (i) fabrication of the membrane from dimethylacetamide (DMAc) solution followed by soaking in phosphoric acid (PA),[10,11,18,19] (ii) via a sol−gel process by direct casting of the high molecular weight PBI solution in polyphosphoric acid (PPA),[20,21] and (iii) from a thermoreversible gel of PBI in PA.[22] The major challenges of these approaches are to obtain a membrane that will show a very high acid doping level and moderately good mechanical stability. It has been shown that with increasing acid doping level, the mechanical stability becomes poor. Therefore, a trade-off between these two important parameters has to be maintained for preparing a superior quality membrane. Hence, there is an opportunity to prepare new PBIs having a variety of polymer backbone structures which could probably enhance the acid-doping level capacity without compromising the mechanical stability. Also, it would be a good addition to the PBI-type polymer system if polymers having different photophysical properties are synthesized, which may serve as potential applicants for the sensor materials.

Until now, a large variety of PBI polymers have been synthesized and studied. Among these, the commercially available PBI, poly[2,2′-(*m*-phenylene)-5,5′-benzimidazole] (known as *m*-PBI), is being widely used. Others include poly(2,5-benzimidazole) (i.e., AB-PBI),[23] pyridine-based PBI

* To whom correspondence should be addressed. Phone: (91) 40 -23134808. Fax: (91) 40-23012460. E-mail: tjsc@uohyd.ernet.in.

10.1021/jp073973v CCC: $37.00 © 2007 American Chemical Society
Published on Web 10/03/2007

SCHEME 1: Synthesis of *m*-Polybenzimidazole-*co*-*p*-Polybenzimidazole (*m*-PBI-*co*-*p*-PBI)

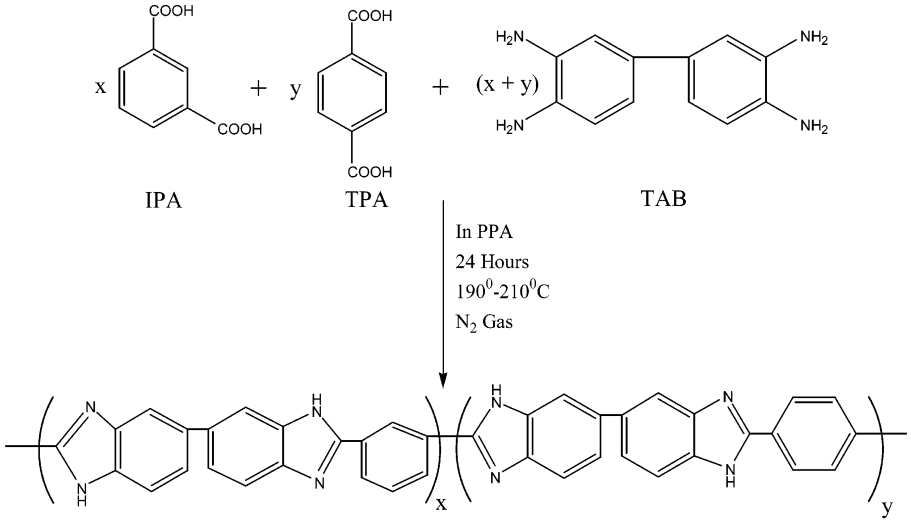

m-*co*-p PBI; x = 0 is p-PBI , y = 0 is m-PBI.

homopolymer,[21] sulfonated PBI,[24] hyperbranched polybenzimidazole (HPBI),[25] naphthalene-based PBI,[26] fluorinated PBI,[27] PBI with a sulfone group or sulfonic acid group in the backbone, etc.[28] Although excellent thermochemical and mechanical stability make the PBI valuable for industrial application, the major drawback is their processibility arising due to poor solubility and infusibility. Much effort has been exercised in the literature to improve the processibility without sacrificing the brand PBI properties. For this purpose, several attempts have been made through the modification of the polymer backbone as well as the side chain.[29] Many investigators have incorporated flexible spacers such as methylene and aryl methylenes, arylamide, and ether linkages in the polymer backbone.[30] Recently, Persson et al. have synthesized ABA triblock copolymers having benzimidazole tethered end blocks with enhanced solubility.[31]

Earlier studies indicate that the molecular weight of the PBI polymers has great impact on their properties, in particular mechanical properties and acid-doping level capacity. Therefore, there is a demand for the preparation of high molecular weight PBI and obviously the best way to do that is to synthesize various polymer backbone structures. However, one should not heavily compromise the solubility issue aiming to increase the molecular weight. In a recent article we have demonstrated the aggregation behavior of the PBI chains in solution through spectroscopic studies.[14] Hence, the synthesis of new polymers with tunable spectroscopic characteristics is desired. Keeping these in mind, we hypothesize that incorporation of the *p*-phenylene linkage in the *m*-PBI backbone would probably be the right track to meet the above targets. Also, we would expect a more structurally symmetrical backbone resulting from the introduction of the para linkage, which in turn enhances the conjugation and flexibility of the polymers. Therefore, in the present study, we report the synthesis of a series of *m*-phenylene−*p*-phenylene based polybenzimidazole random copolymers. The synthesized polymers are characterized by determining inherent viscosity (IV) as a measurement of polymer molecular weight, thermogravimetric analysis (TGA) for the thermal stability, and differential scanning calorimetry (DSC) for the thermal transitions. Fourier transforms infrared (FT-IR) and proton NMR techniques are used to establish the polymer structure. Also, spectroscopic studies such as absorption and fluorescence are carried out to demonstrate the effect of copolymerization on the photophysical properties. Finally, we have studied the wide-angle X-ray scattering (WAXS) to look into the crystalline character of these polymers.

2. Experimental Sectiom

2.1. Materials. 3,3′,4,4′-Tetraaminobiphenyl (TAB) and polyphosphoric acid (115%) were received from Sigma-Aldrich. Isophthalic acid (IPA) and terephthalic acid (TPA) were purchased from SRL, India. Sulfuric acid (98%) and deuterated dimethyl sulfoxide (DMSO-d_6) were received from Merck, India. Dimethylacetamide (HPLC grade) was purchased from Qualigens (India). All chemicals were used as received without further purification.

2.2. PBI Synthesis. An equal number of moles of TAB and either IPA or TPA were taken into a three-necked flask with polyphosphoric acid (PPA) for homopolymers synthesis. IPA and TPA were used to prepare 100% *m*-PBI and 100% *p*-PBI, respectively. For random copolymers (Scheme 1) synthesis the mole fraction of the diacids (IPA and TPA) in the reaction mixture was varied from 10% to 90% but maintaining the total moles of diacids equal to the moles of TAB taken in the reaction mixture along with PPA. The total monomer concentrations were gradually decreased with increasing TPA mole fraction in the mixtures. The reaction mixtures were stirred by an overhead stirrer continuously in nitrogen atmosphere at 190−210 °C for ∼24 h. The PBI polymers were isolated, neutralized with sodium carbonate, washed thoroughly with water, and dried in a vacuum oven at 100 °C for 24 h. The dried polymers were kept in a vacuum desiccator for further characterizations.

2.3. Viscosity. The viscosity measurements of the polymer solutions in H_2SO_4 (98%) were carried out at 30 °C in a constant temperature water bath, using a Cannon Ubbelohde capillary dilution viscometer (model F725), and the inherent viscosity (IV) values were calculated from the flow time data. For all the flow time measurements 0.2 g/dL of polymer solution in H_2SO_4 (98%) was used.

2.4. IR and NMR Spectroscopy. The IR spectra of the samples were recorded on a (JASCO-5300) FT-IR spectrometer. The experiments were carried out at room temperature on PBI films having a thickness of 40 μm. All the NMR spectra of the PBI solutions in DMSO-d_6 were recorded with a Bruker AV 400 MHz NMR spectrometer at room temperature.

2.5. Thermal Study. Thermogravimetric and differential thermal analysis (TG-DTA) were carried out on a (Netzsch STA

TABLE 1: Various Reaction Parameters of PBI Random Copolymers

para content (mol %)	monomer concn[a] (wt %)	inherent viscosity[b] (dL/g)
0	4.83	0.621
10	4.75	1.151
25	3.85	1.111
50	3.7	1.699
75	3.6	1.527
90	3.4	1.621
100	3	1.772

[a] Figure 1 copolymers have been synthesized by using the corresponding monomer concentrations. [b] When the monomer concentrations for the synthesis of all the copolymers were kept constant at 4.83 wt %.

409PC) TG-DTA instrument from 50 to 900 °C with a scanning rate of 10 deg/min in the presence of nitrogen flow. A differential Scanning Calorimeter (Pyris Diamond DSC, Perkin-Elmer) was used to find the glass transition temperature (T_g) of the PBI samples. Approximately 7−10 mg PBI samples were taken in an aluminum pan that was tightly crimped with the help of a DSC crimpier and then scanned from 50 to 500 °C at a heating rate of 10 deg/min in the presence of constant nitrogen gas purging. The DSC was calibrated with use of standard In and Zn before the PBI samples were scanned.

2.6. Absorption and Fluorescence Spectroscopy. Electronic absorption spectra were recorded on a Shimadzu model UV-3100 UV−visible spectrometer. Steady-state fluorescence emission spectra were recorded on a Jobin Yvon Horiba spectrofluorimeter (Model Fluoromax-3). PBI samples were dissolved in dimethylacetamide (DMAc) and the spectra were recorded. For determination of the fluorescence quantum yield (Φ_f) of the PBI samples quinine sulfate ($\Phi_f = 0.546$ in 1 N sulfuric acid) was used as a reference.

2.7. X-ray Diffraction. The X-ray diffraction (XRD) patterns of the dry PBI powders were collected in a Philips powder diffraction apparatus (model PW 1830). The powders were taken in a glass slide and the diffractograms were recorded with use of nickel-filtered Cu Kα radiation at a scanning rate of 0.6° 2θ/min.

3. Results and Discussion

3.1. Synthesis and Molecular Weight Control. A series of *m*-polybenzimidazole−*p*-polybenzimidazole random copolymers (*m*-PBI-*co*-*p*-PBI) have been synthesized and the polymer backbone structure is shown in Scheme 1. We have varied the composition of meta and para structures in the copolymer from 10% to 90% by changing the mole ratio of IPA and TPA, respectively, in the initial reaction mixture. Also, 100% meta homopolymer and 100% para homopolymer are prepared taking the respective diacid with the TAB. In all the polymerization processes the stoichiometric balance between the TAB and the diacids is well maintained. Also, the reaction conditions for all the reactions are similar except the initial monomer concentration in the reaction mixture. Inherent viscosity (IV) is a measure of the molecular weight of the polymer; a higher IV value indicates a higher molecular weight.[32] The molecular weight of PBI has in the pertinent literature been expressed in terms of IV, measured on sulfuric acid solution.[9,33] The monomer sensitivity to the polymerization conditions has a more significant influence on the viscosity behavior than that of the monomer structure.[33] Table 1 and Figure 1 show that low monomer concentration in the reaction mixture is required to prepare higher para content copolymer. We have also carried

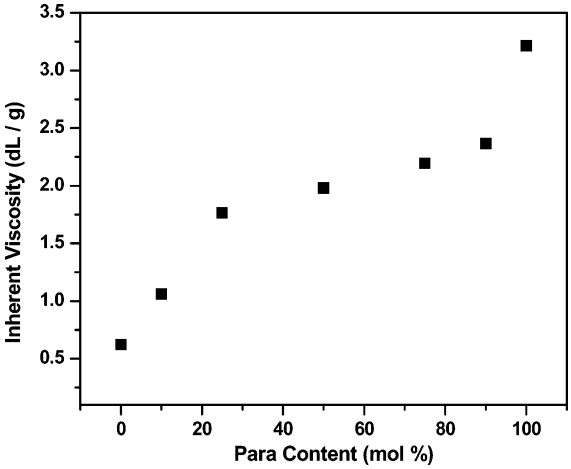

Figure 1. Variation of molecular weight (inherent viscosity) with para content of the PBI copolymer.

out the polymerizations with same monomer concentration (4.83 wt %) to prepare all the copolymers. But such reactions produce low inherent viscosity (IV) polymers, in particular when the para content in the polymers keeps on increasing (Table 1). This observation proves the importance of the variation of the monomer concentration in the reaction mixture to achieve higher molecular weight PBI. We believe that the solubility of the TPA in PPA plays a major role for the polymerization. With the solubility of TPA in PPA being very low[34] when the monomer concentration is high (4.83 wt % in Table 1), more and more TPA is precipitating out from the reaction mixture as insoluble solid destroying the stoichiometric balance. This in turn disfavors the reaction equilibrium and yields low IV polymers. Figure 1 is a plot of the inherent viscosity (IV) against the para content of the copolymers. The inherent viscosity values of these copolymers could be compared to one another as a measure of their molecular weights since both the meta and para portions have identical weights and the only difference in the polymer structure is the isomeric phenyl moiety. Figure 1 clearly shows the effect of para content on the molecular weight of the polymer; with increasing para content the molecular weights increase. Hence, changing the carboxylic acid group position in the diacid from meta to para enhances the molecular weight enormously and allows us to control the molecular weight by preparing the appropriate copolymer. The solubility of benzene dicarboxylic acids in polar acidic solvents depends upon the position of the carboxylic groups in the benzene ring. The poor solubility of dicarboxylic acid is observed with the carboxylic groups which are far apart in the benzene ring because acid groups are probably unable to form the internal dimmers through hydrogen bonding interaction between carboxylic groups of the same acids or coming from two different molecules of the acid.[35,36] Thus TPA (1,4-) has lower solubility than IPA (1,3-) in acidic solvents. The reason behind the formation of higher molecular weight polymer with increasing para content can be explained by considering the extremely low solubility of TPA in PPA.[34] Because of the poor solubility of TPA in the reaction mixture, the growing polymer chain (oligomer) ends consist of the soluble monomer TAB. This is clearly proved by the absence of any carboxylic phosphate ester or acid amide group in the oligomeric radicals isolated from the reaction mixture at different time intervals. The absence of carbonyl stretching at ∼1710 cm^{-1} in the IR spectra of the oligomer radical presented in Figure 1 in the Supporting Information supports our argument. These oligomeric chain ends quickly react further with the dissolved TPA in the mixture and the reaction continues. As

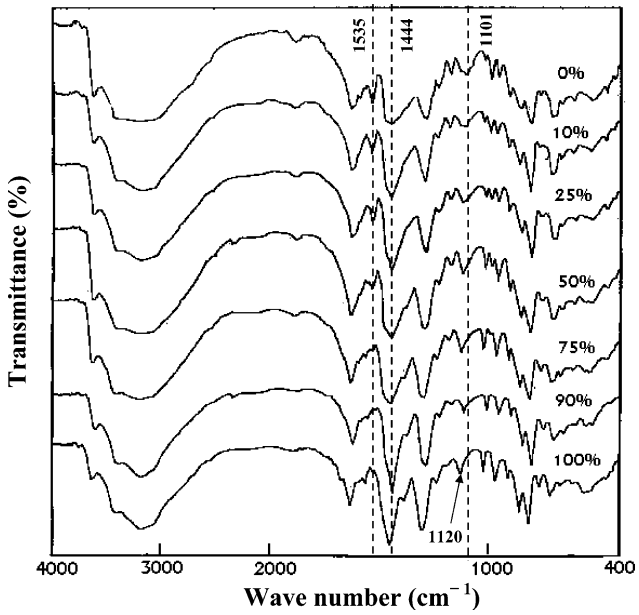

Figure 2. FT-IR spectra of all the PBI polymers. Para content (mol %) of the polymers is indicated in the figure.

soon as the deficiency of TPA arises in the solution owing to its low solubility in PPA, more and more TPA dissolution takes place to maintain its saturation concentration and polymerization keeps on going producing bigger molecules. A similar type of observation was reported earlier in the case of polybenzoxazoles.[34,37] It is also interesting to note that the para structure of the diacid monomer introduces more symmetry in the polymer backbone. Hence, we hypothesize that molecular weight control and symmetry in the polymer backbone will help us to tune the molecular property, which is discussed in the following sections.

3.2. IR and NMR Spectroscopy. The IR spectra of all the PBI polymers are recorded on the thin film made from the dilute solution of the polymers in dimethylacetamide (DMAc) and are presented in the Figure 2. Before recording the IR spectra, the films are boiled in hot water and dried in a vacuum oven at 100 °C for 2 days to remove any traces of DMAc. In Figure 2 the absence of C−H stretching of CH_3 at 2940 cm^{-1} for DMAc indicates the efficiency of our drying process. PBI is slightly hygroscopic and it can absorb moisture up to 5% of its weight readily;[38] therefore O−H stretching at 3616 cm^{-1} is expected. The presence of O−H stretching of H_2O at 3616 cm^{-1} in all the spectra (Figure 2) indicates this fact. The IR spectra presented in Figure 2 for different PBI polymers are quite similar and the majority of the bands are for the characteristic stretching of PBI. These bands have been widely discussed earlier by several authors.[28,39,40] However, it is worth noting that the bands at 1536, 1444, and 1101 cm^{-1} indicated by the dotted line in the Figure 2 are not identical for all the samples. Previously, the bands at 1536 and 1444 cm^{-1} were assigned as in-plane ring vibration of 2-substituted benzimidazole and 2,6-disubstituted benzimidazole, respectively.[39] From Figure 2, it is evident that the band at 1536 cm^{-1} becomes less intense with increasing para content in the polymer chain and almost nonexistent for 100% *p*-PBI. On the other hand, the peak at 1444 cm^{-1} becomes more intense gradually with increasing para content. These deviations in the band intensities of the PBI polymers are obviously due to the substitution in the 2-position of the benzimidazole ring, which arises because of the different polymer backbone structure prepared by copolymerization. Another non-identical behavior of the different polymers is observed at the 1101 cm^{-1} band, which is shifted gradually to higher frequency with increasing para content. For 100% para, the band appears at 1120 cm^{-1}. This band is assigned as N−C stretching coupled with the stretching of adjacent bonds in the molecule and the position of the absorption depends on the pattern of the substitution on the α-carbon atom.[41] Upon copolymerization, the substitution pattern on the α-carbon atom varies, which results in the shifting of the band from 1101 to 1120 cm^{-1}. The introduction of para substitution in the polymer chain brings more flexibility and symmetry in the polymer backbone and it interferes with the vibration characteristics; therefore the N−C−C coupled vibration takes place at higher frequency. Hence, IR spectroscopy is found to be an efficient tool to demonstrate the effect of copolymerization and the polymer backbone structure.

Though IR study proves the structure of the copolymer qualitatively, it does not elucidate the copolymer backbone structure quantitatively. Rather the proton NMR study is more useful and it has been used extensively before in the literature to look into the copolymer structure and determine the copolymer composition more precisely.[24,28,42] Figure 3 shows the chemical structure of the copolymer, proton NMR spectra of all the copolymers, and the peak assignments of the NMR spectrum. The peak assignments presented in the Figure 3 are in good agreement with the anticipated chemical structure. The imidazole proton signals for the meta and para portions of the chain, denoted as H_a and H_b, are observed at around 13.26 and 13.15 ppm, respectively. Both signals are observed almost in the same region as expected; however, the slight downfield shift of the H_a proton is because of the different chemical environment of the meta structure compare to that of the para structure. In addition, three distinguishable peaks are observed, denoted as H_f, H_g, and H_h at 9.15, 8.32, and 8.42 ppm. The H_f and H_g signals are purely due to the meta structure and the H_h signal is for the para structure. From Figure 3, it is evident that the intensity of the characteristic meta signals (H_a, H_f and H_g) is decreasing and the para responsive signals (H_b and H_h) are increasing with increasing para content in the polymer chain. For example, the intensity of the H_a and H_b signals for the 50% para sample is almost the same indicating the 50:50 compositions. This observation indicates that the copolymerization has taken place successfully and the ratio of the meta and the para mole fraction in the samples can be quantified. The percentages of the meta and the para mole fraction in the samples are calculated from the integral ratio of the proton peaks H_a, H_b, H_f, H_g, and H_h. We have calculated the percent of the para mole fraction in the samples from the proton NMR spectrum using eq 1 and these values are given in the Table 2.

$$\text{para mole fraction (\%)} = \frac{H_b + H_h}{H_a + H_b + H_f + H_g + H_h} \times 100 \quad (1)$$

Table 2 lists the contents of the para units in the series of copolymers. All the values are in good agreement with the monomer feed ratio taken in the initial reaction mixtures, which thus suggests that all the starting monomers are successfully incorporated into the copolymer chains. Also, it is evident that the meta and para composition in the copolymer chains can be readily controlled by changing the molar feed ratio (IPA:TPA) at the start of the polymerization.

However, a critical observation of the Table 2 data brings our attention to a moderate deviation in the para composition from the monomer feed, in particular for the higher para content copolymer. We have presented in the Table 2 data graphically

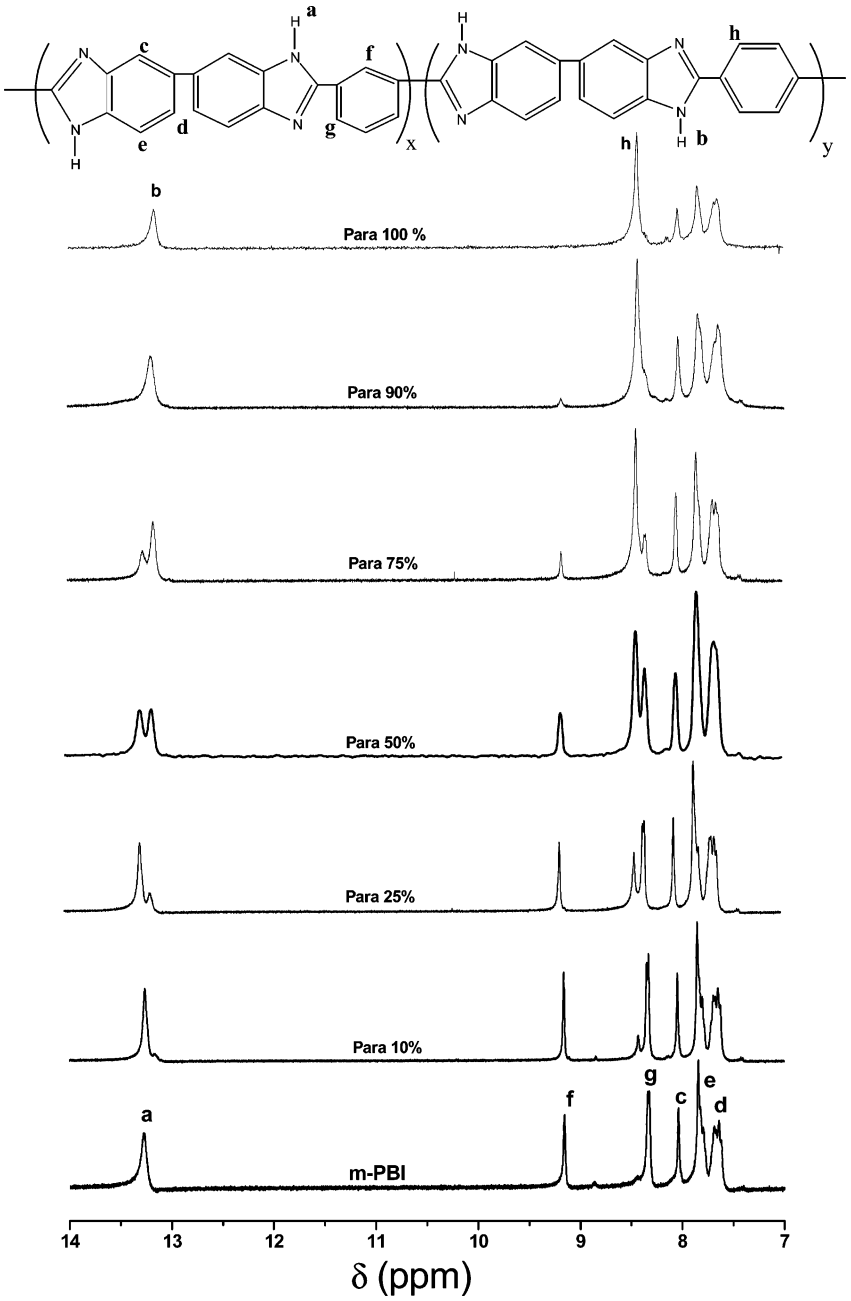

Figure 3. The chemical structure, proton NMR spectra of all the copolymers, and the peak assignments of the NMR spectrum.

TABLE 2: Comparison of the Expected Para Content of the Copolymers Based on TPA Feed in the Reaction with Measured Para Content Calculated from Proton NMR

feed TPA (mol %)	found para content (mol %)
0	0
10	11.25
25	26.61
50	51.52
75	78.05
90	97.60
100	100

shown in Figure 4 to look at the type of deviation. Figure 4 shows a positive deviation (solid line) from the anticipated linearity (dotted line) based on the monomer feed in the polymerization mixture. This kind of behavior is unusual for the step growth polymerization since step reactions are carried out to close to 100% conversion for the synthesis of high

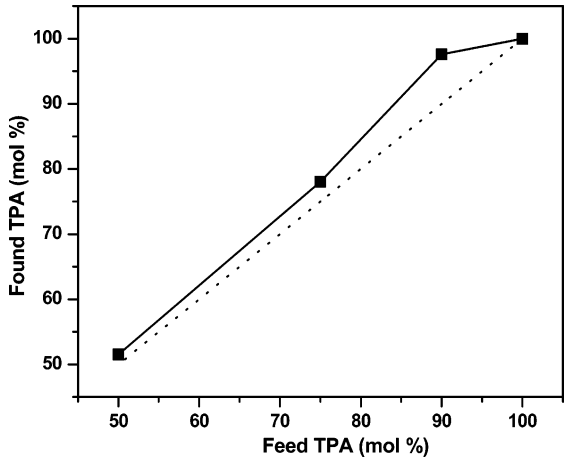

Figure 4. Deviation of comonomer composition in PBI copolymers measured by proton NMR spectroscopy.

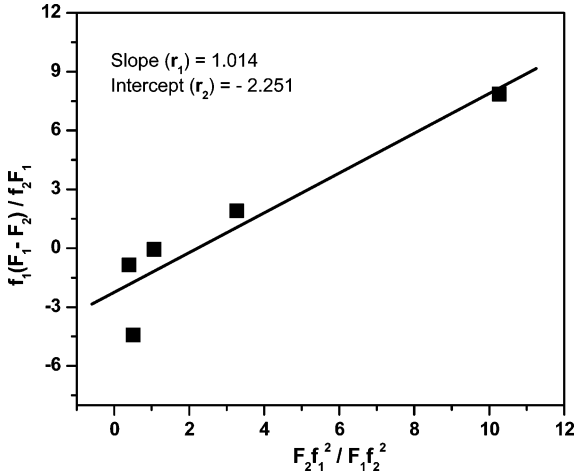

Figure 5. Plot for calculating reactivity ratios of monomers (IPA and TPA) by using eq 2.

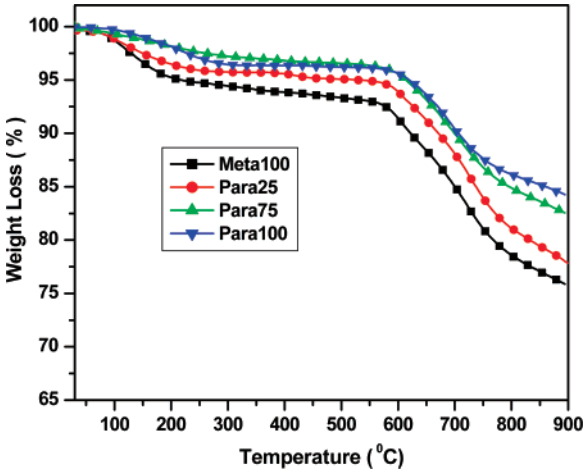

Figure 6. TGA curves of the PBI polymers. Para content (mol %) of the polymers is indicated in the figure.

TABLE 3: Thermal Stability Data of All the PBI Polymers

para content (mol %)	$W_{570°C}$ (%)[a]	$T_{10\%}$ (°C)[b]	$W_{890°C}$ (%)[c]
0	92.8	621	75.9
10	94.8	654	78.1
25	94.5	667	79
50	95.5	680	79.1
75	96.2	696	82.6
90	96.2	698	83.3
100	96.2	707	84.5

[a] Residual weight percent at 570 °C. [b] Temperature at which the 10% weight loss is observed. [c] Residual weight percent at 890 °C.

molecular weight polymers and step polymerizations are equilibrium reactions. A few earlier studies on copolycondensation showed the deviation in composition.[43,44] In the present system because of the large difference in solubility of the IPA and TPA in PPA,[34,37] deviation in the copolymer composition from the monomer feed is expected. This observation gives a hint that probably the rates of the reactions of the monomers are not similar and hence the reactivity ratios of the monomers are different. On the basis of this argument, it was thought necessary to obtain the reactivity ratios of the comonomers. A simple kinetic scheme for copolymerization is used to discuss the rates of the reactions of the monomers.[44] The M_1 and M_2 represent the IPA and TPA monomers, respectively. The asterisk in the prefix indicates the growing polymer chain. The four possible reaction sequences are the following:

$$M^*_1 + M_1 \xrightarrow{k_{11}} M_1M^*_1$$

$$M^*_1 + M_2 \xrightarrow{k_{12}} M_1M^*_2$$

$$M^*_2 + M_1 \xrightarrow{k_{21}} M_2M^*_1$$

$$M^*_2 + M_2 \xrightarrow{k_{22}} M_2M^*_2$$

The rate constants of the respective reactions are denoted by "k" with appropriate sign in the suffix. We have calculated the reactivity ratio of IPA and TPA using the well-known Fineman and Ross[45] procedure (eq 2) from the proton NMR data. Fineman and Ross rearranged the Mayo and Lewis[46] equation as

$$\frac{f_1(F_1 - F_2)}{f_2F_1} = \frac{F_2}{F_1}\left(\frac{f_1^2}{f_2^2}\right)r_1 - r_2 \qquad (2)$$

where f_1 and f_2 are the mole fraction of the monomer IPA and TPA respectively in the feed of the copolymerization, with F_1 and F_2 being their instantaneous compositions (mol fractions) in the copolymer. A plot (Figure 5) of the left-hand side (LHS) of eq 2 against $F_2/F_1(f_1/f_2)^2$ results in a straight line with slope equal to r_1 and intercept equal to $-r_2$, where r_1 and r_2 are the reactivity ratios of the monomer IPA and TPA, respectively. The reactivity ratios are defined as $r_1 = k_{11}/k_{12}$ and $r_2 = k_{22}/k_{21}$. From Figure 5 the reactivity ratios obtained for IPA (r_1) and TPA (r_2) are equal to 1.014 and 2.251, respectively. The reactivity ratio of TPA being greater than unity and larger than that of IPA reveals that the TPA oligomers preferentially add TPA monomers instead of IPA monomers. Hence at higher para content copolymers the actual para content is more than the feed, which explains the positive deviation in Figure 4. In comparison, the reactivity ratio of IPA (r_1) is equal to unity and less than that of TPA. This indicates that the IPA monomer is not biased toward IPA as that of TPA. Hence we do not observe any deviation in Figure 4 for the higher meta composition or the lower para composition of the copolymers. The r_2 is 2.22 times bigger than r_1 ($r_2/r_1 = 2.22$), therefore TPA is 2.22 times more reactive than IPA toward TAB. Thus from the above results it is clear that during polymerization the TPA monomer is being consumed faster rate than the IPA monomer.

3.3. Thermal Study. The thermal stabilities of the synthesized PBI samples are performed under nitrogen atmosphere at a heating rate of 10 deg/min. The representative TGA curves for four different samples are shown in the Figure 6 and the thermal behavior data for all the samples are presented in Table 3. Two distinct different weight losses are observed from Figure 6. An initial weight loss at around 100−120 °C and a second weight loss at around 570−600 °C are observed. The first weight loss is assigned to the loss of loosely bound absorbed water molecules.[24] All the samples used for studying the TGA and IR are subjected to exhaustive drying in a vacuum oven at 100 °C. Despite this drying process, we have observed the weight loss due to absorbed water in TGA (Figure 6) and O−H stretching for water molecules in the IR (Figure 2). These observations indicate that PBI absorbs moisture readily and it absorbs moisture even during the sample handling time, which also supports the earlier report that PBI can absorb ~5% (by weight) moisture very easily from the atmosphere.[39] The

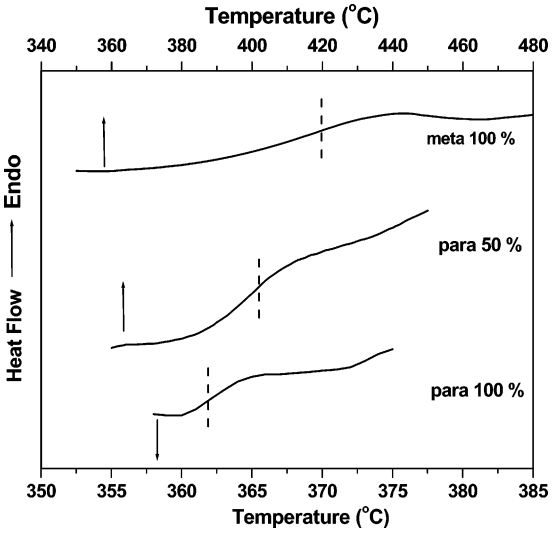

Figure 7. DSC thermograms of PBI polymers. Arrows indicate the temperature axis and the horizontal dotted lines represent the glass transition temperatures.

degradation of the polymer backbone is responsible for the second weight loss at ~570 °C.[20,47] For all the PBI polymers heating to ~570 °C results in only <10% weight loss (Table 3) indicating the remarkable thermal stability of the polymers. Though an earlier report[33] suggests identical thermal stability of both the meta and the para structure, we have observed that significant differences in the thermal stability exist owing to the *m*- and *p*-phenylene groups in the chain. Table 3 shows that the $T_{10\%}$ (temperature at which 10% weight loss is observed) increases as the para content increases in the polymer chain. Furthermore, the weight loss at the final temperature, viz., 890 °C, becomes less for higher para content (Table 3). These observations clearly suggest that the introduction of *p*-phenylene groups in the polymer backbone enhances the thermal stability of the polymer.

The glass transition temperatures of all the polymer samples are measured by using a differential scanning calorimeter (DSC). The DSC measurements show that the glass transition temperatures (T_g) of the *m*-PBI and the *p*-PBI are 420 and 361 °C, respectively (Figure 7). In the literature, the T_g value of the *m*-PBI is reported by several authors. The reported values are between 400 and 450 °C depending upon the measurement techniques followed and the molecular weight of the sample.[48,49] Therefore, our T_g value of the *m*-PBI is in agreement with the reported observations. To our knowledge until now no efforts have been made to measure the T_g of the *p*-PBI. The T_g of the *p*-PBI is 59 °C lower than that of the *m*-PBI, which indicates that the *p*-PBI backbone is more flexible than the *m*-PBI chains. The flexibility in the *p*-PBI backbone arises because of the presence of better conjugation between the imidazole ring and the *p*-phenylene linkage. From Figure 2, IR studies show that the coupled N−C−C linkage vibrates at a higher frequency for the *p*-PBI than the *m*-PBI indicating the presence of the double bond nature in the *p*-backbone. Moreover, para substitution in the polymer chain brings more symmetrical arrangement in the backbone. The flexibility and the symmetrical nature of the para backbone enhance the segmental mobility of the chains and hence show a lower glass transition temperature compare to the meta structure.[50] Figure 7 shows the representative DSC curves for various copolymers along with the two homopolymers. All the DSC curves for the homopolymers and the copolymers show a single T_g transition as observed in Figure 7. Also, we have measured the T_g of the copolymers from the tan δ vs temperature plot obtained from the dynamical mechanical analysis (DMA) as shown in Figure 2 in the Supporting Information. The DMA and DSC results are tallying each other quite well. The glass transition temperatures of the copolymers first decrease slowly and then steadily with the increase in para content as presented in Figure 8. The expected T_g of the random copolymers are estimated by the Fox equation (eq 3) as follows:

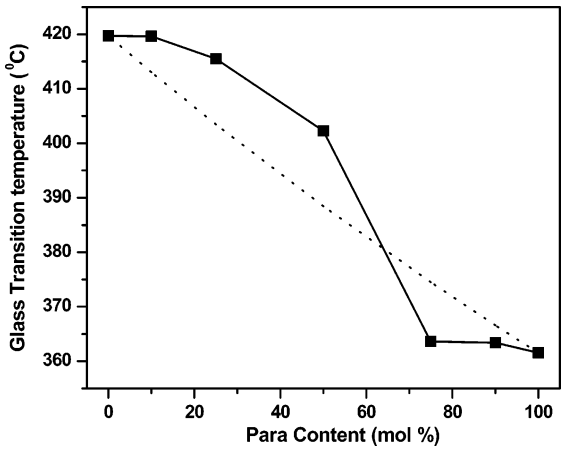

Figure 8. Variation of glass transition temperature (T_g) with para content of the PBI copolymers. The solid line is experimentally obtained and the dotted line is calculated from the Fox equation.

$$\frac{1}{T_g} = \frac{w_1}{T_{g1}} + \frac{w_2}{T_{g2}} \tag{3}$$

where w_1 and w_2 are the weight fractions and T_{g1} and T_{g2} are the glass transition temperatures of the two homopolymers. Figure 8 shows that the experimental T_g values obtained from the DSC measurements (solid line) deviate from the calculated values obtained from the Fox equation (dotted line). The positive deviation is observed for the higher meta content whereas the negative deviation is exhibited by the higher para content polymers. The positive deviation from the linear additive rule (eq 3) for the higher meta content region could be due to the intrachain steric hindrance arising from the less symmetrical meta structure. The negative deviation for the higher para content region can be explained in the light of the reactivity ratio of the TPA. Since the TPA reactivity ratio is bigger (2.251) and greater than unity, therefore higher para content copolymers contain more and more para segments and exhibit lower T_g than the anticipated T_g by the Fox equation.

3.4. Spectroscopy. The absorption and the fluorescence emission spectra of all the PBI polymers are studied from their dilute solution (2×10^{-5} M) in dimethylacetamide (DMAc). The concentration is expressed by considering one repeat unit as 1 mol of PBI. The absorption spectra of the PBI polymers in DMAc are shown in Figure 9. Each spectrum shows distinct $\pi \rightarrow \pi^*$ transition peaks above 340 nm.[12,14] The peak positions are tabulated in Table 4. The gradual bathochromic shift of the $\pi \rightarrow \pi^*$ absorption maxima with increasing para content in the copolymer backbone is observed (Figure 9, Table 4). The 100% *p*-PBI homopolymer absorbs at ~50 nm higher wavelength than the 100% *m*-PBI homopolymer. The introduction of the *p*-(1,4)-phenylene linkage into the polymer backbone enhances the conjugation between the imidazole and the phenylene ring, which results in the above-mentioned bathochromic shift of the $\pi \rightarrow \pi^*$ absorption maxima.[26,33] Therefore, our argument about the increased conjugation in the backbone due to the para

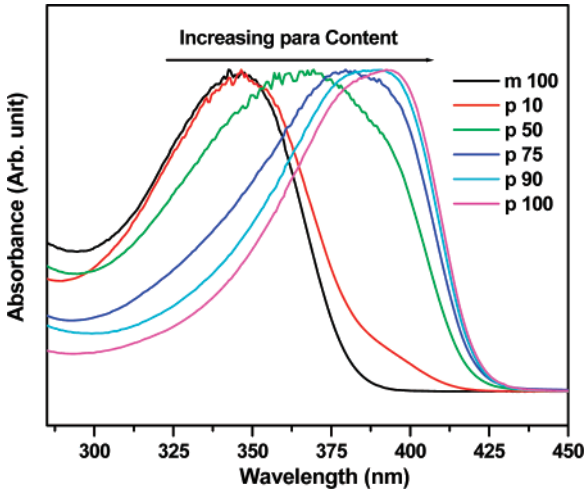

Figure 9. Absorption spectra of the indicated PBI polymers in DMAc solution as recorded with a cuvette of 1 cm path length. Concentrations are 2×10^{-5} M.

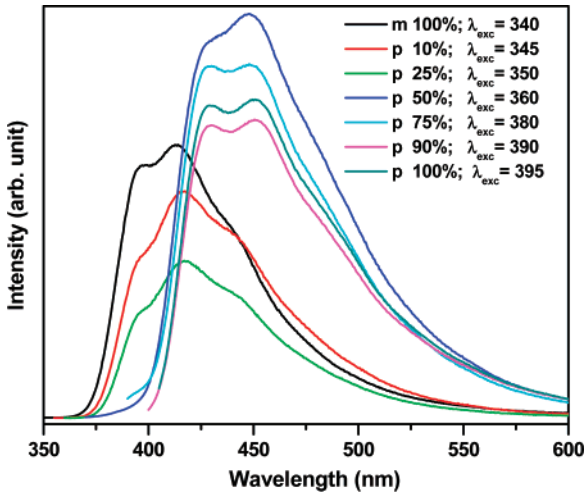

Figure 10. Fluorescence emission spectra of the indicated PBI polymers in DMAc solution. Concentrations are identical to those for Figure 9. Excitation wavelengths (λ_{exc}) are indicated in the figure.

TABLE 4: Electronic Spectroscopy Data of All the PBI Polymers

para content (mol %)	absorption peak (nm)	emission peaks (nm)	Φ_f
0	344	396 416	0.515
10	346	396 416	0.569
25	348	396 416	0.660
50	368	428 450	0.651
75	382	428 450	0.528
90	390	428 450	0.508
100	394	428 450	0.501

substitution using IR spectra and thermal studies discussed in the previous sections is in good agreement with the absorption studies.

The emission spectra of the PBI polymers in DMAc are presented in the Figure 10. The excitation wavelengths (λ_{exc}) are chosen based on the $\pi \rightarrow \pi^*$ absorption maxima shown in Table 4. The concentration of the solution is 2×10^{-5} M, which

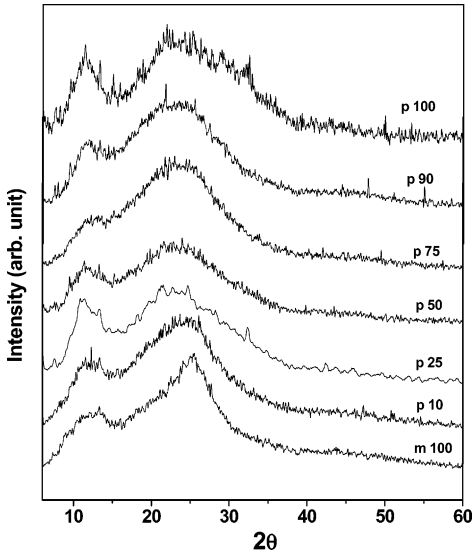

Figure 11. WAXS diffractograms of all the PBI samples.

is kept constant for all cases. The emission wavelengths and the measured fluorescence quantum yields (Φ_f) are presented in Table 4. All the emission spectra of the PBI samples show two fluorescence bands.[12,14] The lower wavelength and the longer wavelength peaks from the excited ^1L_b state in the benzimidazole ring of the PBI are assigned as 0−0 and 0−1 transitions, respectively. The spectral nature and shapes of the bands are similar to those of the earlier reports.[12,14] In a recent report, we have shown a longer wavelength peak at ~548 nm exists for the highly concentrated (5×10^{-3} M) *m*-PBI solution in DMAc due to the excimer/aggregation formation.[14] The concentration (2×10^{-5} M) that we have studied here is much lower than that concentration; hence the absence of the 548 nm band is expected. For the 100% meta homopolymer, 10% para copolymer, and 25% para copolymer the emission peak positions (398 and 416 nm) are the same (Figure 10 and Table 4). However, the emission bands are shifted gradually to the higher wavelength (428 and 450 nm) from the 50% para composition onward and resemble similar behavior of the other higher para content polymers. The shifting of the emission bands toward the longer wavelength also supports the conjugation along the polymer backbone due to the introduction of the *p*-phenylene linkage. This observation once again strengthens our previous argument about the better conjugation of the higher para content sample. The fluorescence quantum yields for all the samples are quite large (Table 4), which indicates that all the PBI samples studied here are highly fluorescent. To our knowledge we are the first to report the fluorescence quantum yield of the PBI polymers. Table 4 shows that the quantum yields for all the PBI samples are almost identical, indicating similar fluorescent behavior. However, 25% and 50% para content samples show little higher quantum yield. This might be due to the existence of their less probable nonradiative pathways.

3.5. X-ray Diffraction. The wide-angle X-ray diffraction (WAXS) patterns of all the PBI samples are presented in Figure 11. From the figure, it is evident that all the samples are amorphous in nature. In all cases two broad peaks at around 13 and 25 2θ (deg) are observed. But, no sharp peak is observed in any of the cases. The existence of the broad peaks results from a convolution of amorphous and crystalline scattering. Earlier several authors reported a similar observation for the PBI-type polymers.[22,26,30,49] Therefore, we can conclude that the introduction of the *p*-phenylene linkage in the polymer backbone does not influence the packing capacity of the polymer chains

though it brings more symmetry in the structure. All the polymers studied here are completely noncrystalline and hence we have not observed any crystalline melting peak in the DSC study. We have obtained a single glass transition temperature (Figure 7) because of the amorphous nature of the polymers.

4. Conclusion

We have synthesized and characterized a series of random copolymers of polybenzimidazole consisting of *m*- and *p*-phenylene linkage in the backbone. Higher molecular weight polymers are obtained from higher para content copolymer due to the low solubility of the *p*-phenylene dicarboxylic acid (TPA) monomer. The higher reactivity ratio of TPA than isophthalic acid (IPA) obtained from the proton NMR studies provides the proof for the positive deviation of the copolymer composition from the monomer feed ratio. The thermal stability of the dry polymer powders is increased due to the copolymerization. The introduction of the *p*-phenylene linkage in the backbone enhances the flexibility of the polymer chain and hence T_g decreases with increasing para content in the copolymer. The T_g of the copolymers shows deviation from the expected T_g calculated by the Fox equation. FT-IR study shows that the conjugation along the chain increases in the case of the para structure compare to the meta structure. The bathochromic shift in the absorption spectra and longer wavelength emission for higher para content PBI copolymer in DMAc solution are observed due to such increased conjugation along the chain. All the PBI polymers synthesized here are completely amorphous in nature. In summary we are able to demonstrate that the molecular properties (viz., molecular weight, thermal stability, T_g, and photophysical behaviors) of the PBI-type polymers can be efficiently controlled by copolymerizing the isomers of the dicarboxylic acids with the tetraamine.

Acknowledgment. We gratefully acknowledge financial support by DST (Fast track grant number SR/FTP/CS-49/2005) and the UPE programme of the UGC. We thank Dr. R. Nagarajan and Mr. G. Vikram of the University of Hyderabad for helping us with NMR experiments and helpful discussion.

Supporting Information Available: FT-IR spectrum of oligomer isolated after 2 h of 100% *p*-PBI hompolymerization at 190 °C and tan δ vs temperature plots of various copolymers obtained from DMA (dynamical mechanical analyzer) analysis for determination of T_g. This material is available free of charge via the Internet at http://pubs.acs.org.

References and Notes

(1) *Fuel Cell Handbook*, 6th ed.; EG & G Technical Services, Inc.: U.S. Department of Energy, Washington, DC, November 2002.
(2) Blomen, L. J. M. J. *Fuel Cell Systems*; Plenum Press: New York, 1993.
(3) Gottesfeld, S.; Pafford, J. *J. Electrochem. Soc.* **1998**, *135*, 2651.
(4) Yang, C.; Costamagna, P.; Srinivasan, S.; Benziger, J.; Bocarsly, A. B. *J. Power Sci.* **2001**, *103*, 1.
(5) Hickner, M. A.; Ghassemi, H.; Kim, S. Y.; Einsla, B. R.; McGrath, J. E. *Chem. Rev.* **2004**, *104*, 4587.
(6) Savadogo, O. *J. New Mater. Electrochem. Syst.* **1998**, *1*, 47.
(7) Roziere, J.; Jones, D. J. *Annu. Rev. Mater. Res.* **2003**, *33*, 503.
(8) Kerres, J. *J. Membr. Sci.* **2001**, *185*, 3.
(9) Choe, E. W.; Choe, D. D. In *Polymeric Materials Encyclopedia*; Salamone, J. C., Ed.; CRC Press: New York, 1996.
(10) Savinell, R.; Yeager, E.; Tryk, D.; Landau, U.; Wainright, J.; Weng, D.; Lux, K.; Litt, M.; Rogers, C. *J. Electrochem. Soc.* **1994**, *141*, L46.
(11) Samms, S. R.; Wsmus, S.; Savinell, R. F. *J. Electrochem. Soc.* **1996**, *143*, 1225.
(12) Kojima, T. *J. Polym. Sci.*: *Polym. Phys. Ed.* **1980**, *18*, 1685.
(13) Shogbon, C. B.; Brousseau, J.-L.; Zhang, H.; Benicewicz, B. C.; Akpalu, Y. *Macromolecules* **2006**, *39*, 9409.
(14) Sannigrahi, A.; Arunbabu, D.; Sankar, R. M.; Jana, T. *Macromolecules* **2007**, *40*, 2844.
(15) Musto, P.; Karasz, F. E.; MacKnight, W. J. *Macromolecules* **1991**, *24*, 4762.
(16) Deimede, V.; Voyiatzis, G. A.; Kallitsis, J. K.; Qingfeng, L.; Bjerrum, N. J. *Macromolecules* **2000**, *33*, 7609.
(17) Yang, N. C.; Sang, M. L.; Suh, D. H. *Polym. Bull.* **2003**, *49*, 371.
(18) Weng, D.; Wainright, J. S.; Landau, U.; Savinell, R. F. *J. Electrochem. Soc.* **1996**, *143*, 1260.
(19) Mecerreyes, D.; Grande, H.; Miguel, O.; Ochoteco, E.; Marcilla, R.; Cantero, I. *Chem. Mater.* **2004**, *16*, 604.
(20) Xiao, L.; Zhang, H.; Jana, T.; Scanlon, E.; Chen, R.; Choe, E.-W.; Ramanathan, L. S.; Yu, S.; Benicewicz, B. C. *Fuel Cells* **2005**, *5*, 287.
(21) Xiao, L.; Zhang, H.; Scanlon, E.; Ramanathan, L. S.; Choe, E.-W.; Rogers, D.; Apple, T.; Benicewicz, B. C. *Chem. Mater.* **2005**, *17*, 5328.
(22) Sannigrahi, A.; Arunbabu, D.; Jana, T. *Macromol. Rapid Commun.* **2006**, *27*, 1962.
(23) Asensio, J. N.; Borrós. S.; Gómez-Romero, P. *J. Electrochem. Soc.* **2004**, *151*, A304.
(24) Jouanneau, J.; Mercier, R.; Gonon, L.; Gebel, G. *Macromolecules* **2007**, *40*, 983.
(25) Li, Z. X.; Liu, J. H.; Yang, S. Y.; Huang, S. H.; Lu, J. D.; Pu, J. L. *J. Polym. Sci., Part A*: *Polym. Chem.* **2006**, *44*, 5729.
(26) Chen, C. C.; Wang, L. F.; Wang, J. J.; Hsu, T. C.; Chen, C. F. *J. Mater. Sci.* **2002**, *37*, 4109.
(27) Chuang, S.-W.; Hsu, S. L.-C. *J. Polym. Sci., Part A*: *Polym. Chem.* **2006**, *44*, 4508.
(28) Qing, S.; Huang, W.; Yan, D. *Eur. Polym. J.* **2005**, *41*, 1589.
(29) Pu, H.; Liu, Q.; Liu, G. *J. Membr. Sci.* **2004**, *241*, 169.
(30) Scariah, K. J.; Krishnamurthy, V. N.; Rao, K. V. C.; Srinivasan, M. *J. Polym. Sci., Part A*: *Polym. Chem.* **1987**, *25*, 2675.
(31) Persson, J. C.; Jannasch, P. *Chem. Mater.* **2006**, *18*, 3096.
(32) Sun, S. F. *Physical Chemistry of Macromolecules*: *Basic Principles and Issues*; John Wiley & Sons, Inc.: New York, 1994.
(33) Neuse, E. W. *Adv. Polym. Sci.***1982**, *47*, 1.
(34) So, Y.-H. *Acc. Chem. Res.* **2001**, *34*, 753.
(35) Apelblat, A.; Manzurola, E.; Balal, N. A. *J. Chem. Thermodyn.* **2006**, *38*, 565.
(36) Long, B.-W.; Wang, L.-S.; Wu, J.-S. *J. Chem. Eng. Data* **2005**, *50*, 136.
(37) So, Y.-H.; Heeschen, J. P.; Bell, B.; Bonk, P.; Briggs, M.; DeCarire, R. *Macromolecules* **1998**, *31*, 5229.
(38) Brooks, N. W.; Duckett, R. A.; Rose, J.; Ward, I. M.; Clements, J. *Polymer* **1993**, *34*, 4038.
(39) Musto, P.; Karasz, F. E.; MacKnight, W. J. *Polymer* **1993**, *34*, 2934.
(40) Lobato, J.; Cañizares, P.; Rodrigo, M. A.; Linares, J. J.; Manjavacas, G. *J. Membr. Sci.* **2006**, *280*, 351.
(41) Silverstein, R. M.; Webster, F. X. *Spectroscopic Identification of Organic Compounds*; John Wiley & Sons, Inc.: New York, 2002.
(42) Li, Y.; Wang, F.; Yang, J.; Liu, D.; Roy, A.; Case, S.; Lesko, J.; McGrath, J. E. *Polymer* **2006**, *47*, 4210.
(43) Lyoo, W. S.; Kim, J. H.; Ha, W. S. *J. Appl. Polym. Sci.* **1996**, *62*, 473.
(44) Sundarrajan, S.; Ganesh, K.; Srinivasan, K. S. V. *Polymer* **2003**, *44*, 61.
(45) Fineman, M.; Ross, S. D. *J. Polym. Sci.* **1950**, *2*, 259.
(46) Mayo, F. R.; Lewis, F. M. *J. Am. Chem. Soc.* **1944**, *66*, 1594.
(47) Asensio, J. A.; Borrós, S.; Gómez-Romero, P. *J. Polym. Sci., Part A*: *Polym. Chem.* **2002**, *40*, 3703.
(48) Liang, K.; Bánhegyi, G.; Karasz, F. E.; MacKnight, W. J. *J. Polym. Sci., Part B*: *Polym. Phys.* **1991**, *29*, 649.
(49) Kumbharkar, S. C.; Karadkar, P. B.; Kharul, U. K. *J. Membr. Sci.* **2006**, *286*, 161.
(50) Sperling, L. H. *Introduction to Physical Polymer Science*; John Wiley & Sons, Inc.: New York, 1992.